Indian J. Phys. **64B** (3), 213-227 (1990)

Effect of the different parameters governing the stability of drift wave in a magnetized plasma

F F Elashkar
Physics Department, Faculty of Science, Mansoura University, Egypt

Received 31 January 1989, accepted 28 August 1989

Abstract : Influence of the governing parameters, such as electron drift parallel speed, parallel wave length, electron-neutral and ion-neutral collision frequencies, electron temperature and magnetic field, on the stability of drift wave in a magnetized plasma has been studied experimentally and theoretically using a full numerical solution of the exact equation. Drift wave has been excited by a positively biased grid ; at a threshold grid potential secondary excitation and ionisation processes take place in the ejected beam of plasma. Effect of the applied magnetic field on the probability of these processes is discussed. Grid positive potential, electron-neutral collision, parallel wave length, electron temperature and speed are found to be destabilizing, while ion-neutral collision is stabilizing. Using a new parameter β, the effect of magnetic field is investigated and it is destabilizing only up to a certain limit.

Keywords : Instability, drift wave, slab model, cylindrical model.

PACS No : 52.35.Py

1. Introduction

Stability of drift waves has been one of the most commonly investigated phenomena in laboratory plasma (Ellis and Motley 1971 and 1974). Two theoretical models, a slab and a non-local cylindrical models, have been developed (Ellis *et al* 1980) and used to describe drift wave in a weakly ionized and magnetized plasma (Elakshar *et al* 1985). The oscillations were allowed for arbitrary radial dependence and the non-local approximations were made assuming a Gaussian density profile. However, numerous comparison of the non-local cylindrical model, which allows for arbitrary experimental density profile (Ellis and co-workers 1977, 1979 and 1980 and Marden *et al* 1978), have demonstrated the superiority of this model to several less rigorous models (Chen 1967 and Chu *et al* 1969) where density profiles are approximated by Gaussian. In a cylindrical plasma of non-Gaussian density profile, full numerical solution of the exact drift wave equation is essential to compute the parameter $\langle | Q | \rangle$ which represents the effective wave number (equivalent to $K_\perp^2$ in the slab model

and (Q) in the Gaussian cylindrical model). There is no work in the literature dealt with the full numerical solution since Ellis *et al* (1980) and Elakshar *et al* (1985). Moreover, effect of the different plasma parameters on the drift wave stability has been ignored.

In the present work, a mesh grid, biased by D.C. positive potential with respect to anode, was used in the path of the plasma to excite the drift wave. At a certain grid potential, secondary ionisation and excitation processes take place. Similar atomic processes were reported in the literature by Ikazi and Tayler (1970) and Cartier and Merlino (1984). The former used a grid immersed in a plasma where a pulsed potential (=30 volts) was applied, but with no magnetic field. The processes were attributed to the electrons emitted in the plasma by an energy of 30 eV which could ionize or excite the low pressure gas (10^{-4} torr). Influence of magnetic field on the breakdown of low pressure argon and helium discharges was investigated experimentally by Cartier and Merlino (1984), but no explanation was given. It is the purpose of the present paper to investigate the effect of magnetic field on the probability of ionisation and excitation processes. Effect of electron drift speed, parallel to the magnetic field, collisions of the charged particle with neutrals, parallel wave length of the drift wave, electron temperature, grid potential and magnetic field on the stability of the drift wave is also investigated on the bases of the full numerical solution of the non-local cylindrical model.

2. Experimental set-up

A schematic illustration of the axial magnetic field device is given in Figure 1.

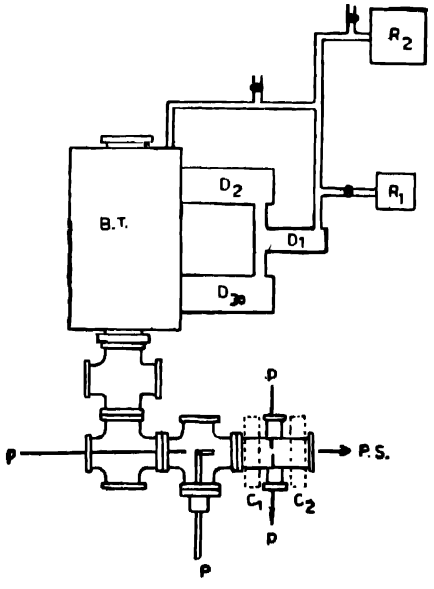

Figure 1. Schematic of the axial magnetic field system. P. S. : Plasma source, C_1 and C_2 : coils, P : probes, D and R diffusion and rotary pumps.

It consisted of a source of steady state plasma (duoplasmatron) and an evacuated metal chamber surrounded by two coils fed with electric current up to 300 Amp. The metal chamber was connected to diffusion pumps and finally to rotary pumps. A fraction of the produced plasma stretched in a beam over a length of 50 cm, enters the magnetic field through the anode aperture and the beam diameter was changed according to the magnetic field strength. The hydrogen plasma characteristics were measured using a single Langmuir cylindrical probe (Swift and Schwar 1970) and a multielectrode probe. The electron temperature (T_e) was between 10 and 6 eV, ion temperature (T_i) between 1.5 – 1 eV and plasma density ranged between 10^{10} and 10^{9} cm^{-3} when the gas pressure was about 10^{-4} torr. Fluctuations of the ion saturation current was used to represent the collective density oscillation characteristic of the drift wave. The oscillations were thus analyzed by an spectrum analyzer and an X-Y plotter. Radially moving probes were used to indicate the radial density and potential profiles and the wave amplitude. Side ports located at the same axial position but differing in azimuth allowed for the determination of the azimuthal mode number (m). A mesh grid was situated in the path of the plasma. A positive, or negative, D.C. bias on this grid was used to excite drift wave.

3. Results and discussion

Plasma potential ϕ_p was determined by three different techniques,

(i) By correcting the floating potential ϕ_f, at a single probe, for sheath voltage using the relation

$$\phi_p = \phi_f + \alpha KT_e/e \tag{1}$$

where α has the nominal value of

$$\alpha = \tfrac{1}{2}\ln(2/\pi\ m_i/m_e)$$

This value is appropriate for a field free plasma, but in a field sufficiently strong that the electron Larmor radius is smaller than the probe radius, α will be reduced to a value of about 2 (Chen 1965).

(ii) By analyzing the I-V characteristics of the single probe (Elakshar and Nossair 1984) : The plasma potential was chosen at the point where the second derivatives of the electron current was zero.

(iii) By using the noise method (Golovanivskii, 1971) : Care was taken to avoid the interference between the used noise frequency (ω_n) and the excited wave frequency of the plasma. The noise frequency was calculated using the formula :

$$J_a/J_\omega = (\omega_n/\omega_p).\omega_c\tau \tag{2}$$

where J_d and J_ω are the displacement and the conduction currents, ω_p is the plasma frequency, ω_c is the electron-cyclotron frequency and τ is the electron collision time (Chen 1974). Typical values of ω_n are 1, 5 and 10 KHz at magnetic fields of 70, 600 and 900 gauss where the displacement current dominates. A noise frequency of 5 KHz was used, which is far below the drift wave frequency. Radial potential profiles are shown in Figures 2a and 2b for magnetic fields of 72

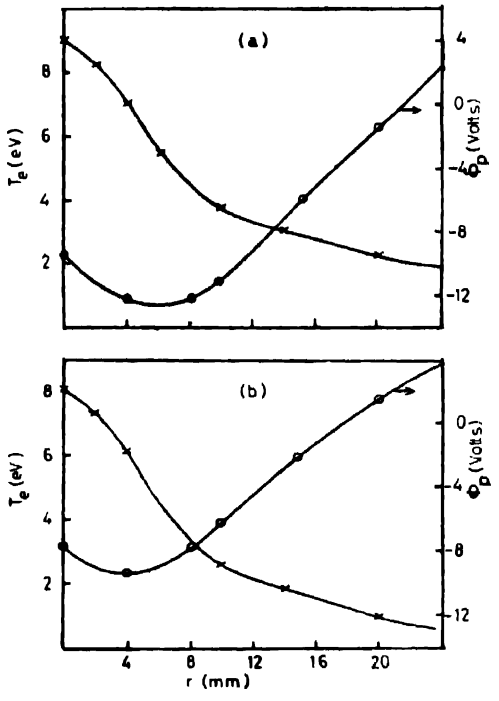

Figure 2. Radial distribution of plasma potential (ϕ_P) and electron temperature (T_e) at (a) 72 gauss and (b) 600 gauss.

and 600 gauss respectively. The radial electron temperature distributions are also shown. For plasma potential ranged from -13 to about $+4$ volts electron temperature decreased from 9 to 2 eV at 72 gauss and from 8 to 1 eV at 600 gauss. The radial profiles of the electron temperature are similar to those of the density (Figures 3a and 3b) and the maximum temperature gradient is about 5 eV/cm.

In Figure 3a, the experimental radial density profile at 72 gauss is compared with a Gaussian density profile, $N=N_0 \exp(-\gamma^2/\gamma_0^2)$, a bell-shaped profile and a flat-top profile (Ellis et *al* 1980), where $\gamma_0 = a/\text{constant}$, a is the plasma radius and the constant has to be chosen to fit the experimental data. The plasma radius (a) was defined at a radial distance where the drift wave amplitude is minimum. The experimental data fits closely to the Gaussian and the bell-shaped

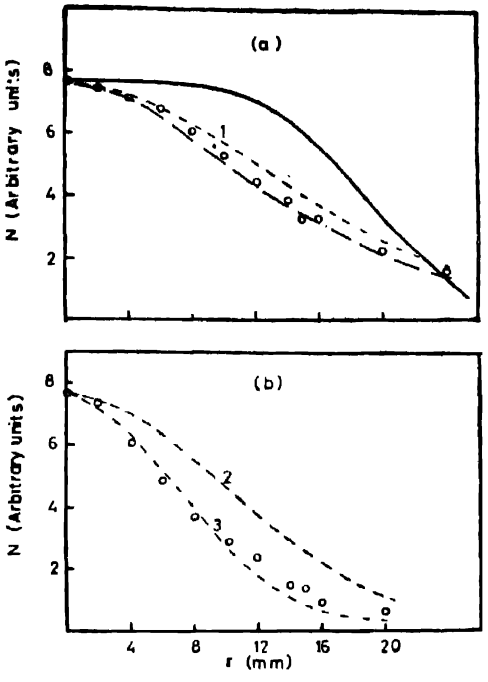

Figure 3. Plasma density profiles at (a) 72 gauss and (b) 600 gauss (o) experimental values, ---- flat top profile, — bell shaped profile and - - - - (1, 2 and 3) Gaussian profiles with r_0 of 2.5, 1.5 and 1.0 respectively.

profiles rather than the flat-top profile. At high magnetic (600 gauss), the measured profile deviated from these profiles as indicated in Figure 3b. Similar profiles were obtained, not shown, at higher gas pressures.

Secondary ionization and excitation processes took place when the mesh grid biased by a positive potential $\geqslant$ a certain value (V_T). Thus V_T is called the threshold potential. Its value raised drasticly at the higher magnetic fields (Figure 4). The plasma density and the light output of the emerged plasma beam were enhanced as a result of these processes. The increment of V_T at high fields is attributed to the change of the probability (P) and the rate coefficient (R) of the secondary processes. The probability (P) is affected by magnetic field according to :

$$P = X.\mathcal{V}_{th}/\mathcal{V}_d.\lambda_{e-n} \qquad (3)$$

where X is the distance travelled by the electrons in the axial magnetic field, $\mathcal{V}_{th}$ and $\mathcal{V}_d$ are the electron thermal and drift velocities respectively and λ is the electron collision mean free path. Measurements of $\mathcal{V}_d$ by modulating the duoplasmatron output using an electrical circuit similar to that used by Bauwens *et al* (1977), showed that its value was doubled (from 1×10^6 to 2×10^6 cm/sec) when magnetic

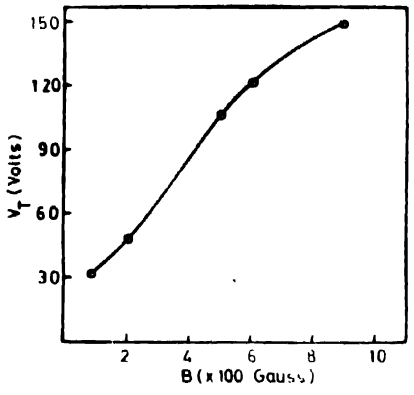

Figure 4. Threshold voltage (V_T), for ionization and excitation, as a function of magnetic field (B).

field was increased three times. Hence the probability (P) was decreased. However, (P) may be enlarged by increasing the thermal velocity $\mathcal{V}_{th}$. Thus to produce secondary processes at high fields the grid potential was raised in order to increase electron energy. Higher rates of excitation and ionisation (R) were also expected at large V_T. (R) was calculated from :

$$R=\int_0^\infty N_e \mathcal{V} Q(\mathcal{V}) d\mathcal{V} / \int_0^\infty N_e d\mathcal{V} \text{ cm}^3/\text{sec} \qquad (4)$$

where $Q(\mathcal{V})$ is the cross section of the atomic process, its value was taken from Massey and Burhop (1969). Eq. (4) was solved numerically, assuming Maxwellian energy distributions. The rates of excitation were (1.3×10^{-8} and 2.9×10^{-8}) and of ionisation were (0.5×10^{-8} and 1×10^{-8}) cm^3/sec assuming the electron temperatures to be 6 and 10 eV respectively. Although Townsend mechanisms are hardly effected by the longitudinal magnetic field (Loeb 1956 and Mitani and Kubb 1960), electron diffusion D is conspicuously decreased by magnetic field B (Okuda and Dawson 1973) D is given by :

$$D=0.0625\ (CKT_e/eB)$$

where C is the light speed.

At low magnetic field (72 gauss) and low grid positive potential ($< V_T$, threshold potential), plasma was stable with $\tilde{n}/n < 1\%$. However, if grid was biased by a potential $\geqslant V_T$, the probe and the spectrum analyzer recorded the onset of a single, coherent mode of the drift wave. Once the plasma was destabilized, grid acts to govern the azimuthal mode numer and frequency of the oscillations. By increasing grid potential, the wave disappeared and a similar oscillations with

higher frequency was onset (Figure 5). Increasing magnetic field (400—900 gauss) caused different modes to onset even at zero or negative grid potentials, but higher frequencies were observed. Typically, drift waves of mode number $m=2$ and frequencies of (45 ± 3), (50 ± 5) and (55 ± 5) kHz were detected at magnetic fields of 400, 600 and 900 gauss respectively when grid potential varied from

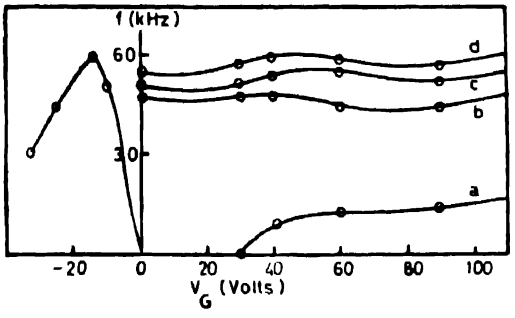

Figure 5. Drift wave frequency f as a function of grid voltage (V_G).

zero to 100 volts (Figure 5). Values of the wave frequency at negative grid potentials, are also enclosed in Figure 5. However, details of these have been explained by Elakshar *et al* (1985).

Using the two fluid equations for a weakly ionized plasma of cold ions and hot electrons (Self 1970) and assuming that : (i) collisional regiem where only electrons or ions collisions with neutral particles are important, (ii) electrons are drifted parallel to the magnetic field at a speed U_0 ; the linear perturbation of the form $\psi(r)\exp(i(k_z Z+m\theta-\omega t)$ results in a second order differential equation for $\psi(r)$ in the form (Ellis *et al* 1980).

$$d^2\psi/dr^2+(1/r+1/n.dn/dr)d\psi/dr+(Q(r)-m^2/r^2)\psi=0 \tag{5}$$

where

$$Q(r)=1/(\omega+i\gamma_i)\rho^2.(\omega^*(r)-(\omega'(r)+i\gamma_i)/\omega-\omega_1+i\gamma_i),$$

$$\omega'(r)=-(KT_e/eB)(m/r)(1/n)(dn/dr),$$

$$\gamma_i=k_z^2KT_e/m_e\gamma_e.$$

$$\rho^2=(KT_e/m_i)/(eB/m_i)^2,$$

$$\psi(r)=e\tilde{\phi}(r)/KT_e$$

$\omega_1=k_zU_0$ and γ_i and γ_e are the ion and electron collision frequencies.

The perturbed part of the density $\tilde{n}(r)$ can also be related to $\psi(r)$ by

$$\tilde{n}(r)=\psi(r)n(r)(\omega'+i\gamma_i)/(\omega+i\gamma_i).$$

For the Gaussian density profile eq. (5) is reduced to (Chen 1967).

$$d^2\psi/dr^2+(1/r-2r/r_0^2)d\psi/dr+(Q-m^2/r^2)\psi=0 \tag{6}$$

For the arbitrary density profile, an average values of $Q(r)$ over the radius can be estimated from :

$$\langle\,|\,Q\,|\,\rangle=\int_0^a \psi^*\,|\,Q\,|\,\psi(r)dr/\int_0^a \psi^*\psi(r)dr \tag{7}$$

For the non-cylindrical model $\langle\,|\,Q\,|\,\rangle$ represents the effective value of $k_\perp^2$ of the local slab model, where $k_\perp^2=2(m/r_m)^2$, m is the mode number and r_m is a radial distance at which $\psi(r)$ is peaked. For a Gaussian profile, Q is estimated as a function of m and r by solving eq. (6) numerically, but for the experimental profiles values of $\langle\,|\,Q\,|\,\rangle$ are computed using eq. (7). For the present study we compute values of $k_\perp^2$, Q and $\langle\,|\,Q\,|\,\rangle$ at two magnetic fields of 72 and 600 gauss. These values were estimated using the experimental profiles in Figures 3a and 3b and Ellis et *al* (1980) foundations. Following eq. (6), the dispersion relation of the drift wave is given by :

$$\omega^2+E\omega+F=0 \tag{8}$$

where

$$E=i\gamma_1(1+1/b)+(i\gamma_1-\omega)$$

and

$$F=\omega_1(\omega-ib\gamma_i)/b-\gamma_1(i\omega+b\gamma_i)/b$$

The real and imaginary parts ω_R and ω_I are thus given by :

$$\omega_R^4+A\omega_R^3+B\omega_R^2+C\omega_R+D=0 \tag{9a}$$

and

$$\omega_I(2\omega_R-W_1)-W_4+W_2\omega_R=0 \tag{9b}$$

When the electron drift speed U_0 is negligable, eqs. (9a) and (9b) are simplified to :

$$G^2+BG+D=0 \tag{10a}$$

and

$$\omega_I(2\omega_R)-W_4+W_2\omega_R=0, \tag{10b}$$

where the parameter $b=k_\perp^2\rho^2$ for the local slab model ($k_\perp^2$ must be replaced by Q or $\langle\,|\,Q\,|\,\rangle$ for the Gaussian or the arbitrary density profiles), $G=\omega_R^2$ and $W_1=\omega_1$. Other factors are listed in the following :

$$W_2 = \gamma_i + \gamma_1(1+1/b),$$

$$W_3 = \omega_1\omega^*/b + \gamma_1\gamma_i,$$

$$W_4 = \gamma_i\omega_1 + \omega^*\gamma_1/b,$$

$$A = -2W_1,$$

$$B = (5W_1^2 + W_2^2 - 4W_3)/4,$$

$$C = (4W_1W_3 - W_1W_2^2 - W_1^3)/4$$

and

$$D = (W_1W_2W_4 - W_1^2W_3 - W_4^2)/4.$$

Eqs. (9) and (10) were solved numerically using the measured plasma parameters e.g. T_e, plasma radius, density profile (Figure 3), wave numbers...etc. Values of ω_R and ω_I, at different magnetic fields, are compared with the non-local predictions in Figures 6a and 6b. Local model predicts lower growth rates

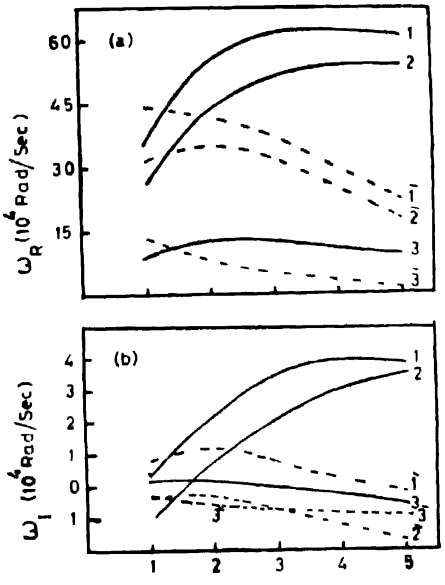

Figure 6. (a) Real frequency (ω_R) as a function of the mode number (m), solid lines 1, 2 and 3 indicate the full numerical solution at (600 gauss and 10^{-4} torr), (600 gauss and 4×10^{-4} torr) and (72 gauss and 10^{-4} torr) respectively. Dotted lines 1, 2 and 3 indicate the local model for the same conditions. (b) Imaginary part (ω_I) for the same conditions as in (a).

ω_I at 600 gauss and stable modes for $m=1-5$ at 72 gauss. The full numerical model confirms the experimental observation that only modes $m=1$ or 2 were unstable. Similar comparison is also shown at high pressure (4×10^{-4} torr)

(Figure 6). Except for $m=1$, the estimated values of ω_R using the local model, are lower than the expected values.

In Figure 7 values of ω_R and ω_I for $m=2$, $B=600$ gauss and $\gamma_{\parallel}=6.4\times10^6$ and 2.4×10^6 sec^{-1}, are shown as a function of the electron drift speed U_0, parallel to the magnetic field. Predictions of the local model have not been shown,

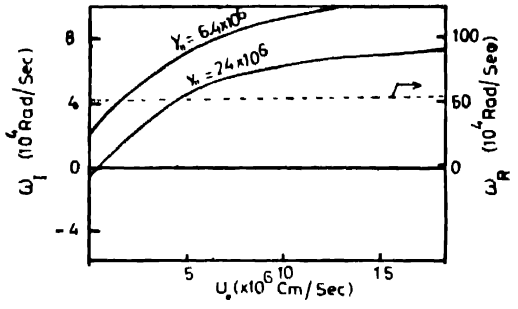

Figure 7. Effect of the electron drift speed (U_0) on the real and imaginary parts of (ω) for two values of the parameter $\gamma_{\parallel}$.

but the dependence on U_0 is very much the same since this parameter does not involve the perpendicular structure of the mode and qualitatively same results are expected, although the quantitative values may be different (Figure 6), and discrepencies may exist. Obviously, the electron drift speed has a strong destabilizing effect and growth rate changed remarkably even for very small increment of U_0. Plasma may be come unstable whenever a weak electron current flows in the beam. Values of the real frequency ω_R are only slight affected by this current. A reasonable explanation for the data in Figure 5 can be derived

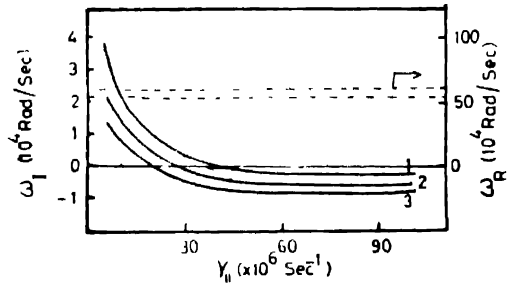

Figure 8. Effect of the parameter ($\gamma_{\parallel}$) on (ω_R), dotted lines and (ω_I) solid lines 1, 2 and 3 for full numerical solution ($m=4$ and 2) and local model ($m=2$) respectively.

as follows ; at low magnetic field (72 gauss), mode is almost stable when grid has lower positive potentials. However, increasing grid voltage would derive a weak current through the machine and increased the electron parallel speed.

Whenever grid voltage reaches the threshold value so that U_0 is high enough, mode becomes unstable. Once plasma is unstable, only slight change in the measured frequency is expected. At high magnetic fields, drift speed increased and unstable modes are detected even at very low grid potential. Therefore, either grid voltage or magnetic field would have the same effect on U_0.

Collisions between charged particles and neutrals are more prevalent than Coulomb collisions in the present experiment. The electron-neutral collision

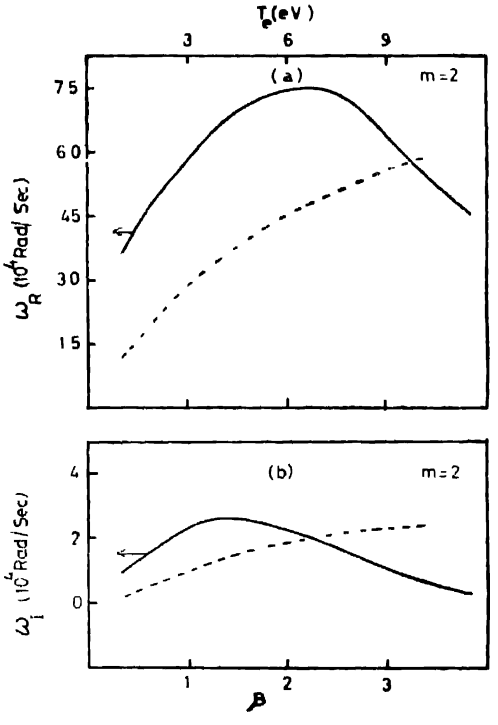

Figure 9. Effect of the parameter (β) and electron temperature (T_e) on (ω_R) and (ω_I) for $m = 2$ and at 600 gauss

frequency γ_e was estimated using the electron thermal velocity and the probability of collision by Brown (1967). Ion-neutral collision frequency γ_i was estimated using Delcroix (1968) tables of limited reduced mobility. Ion collision frequency γ_i is stabilizing factor as predicted by the two models. A considerable decreasing in values of ω_I, and also ω_R, at high gas pressures, i.e. high collision frequency γ_i, is illustrated in Figure 6. The parameter $\gamma_i(=k_z^2.KT_e/m_e\gamma_e)$ was used instead of γ_e since it represents a combination factor of γ_e and the parallel wave length of the drift oscillation λ_z (or k_z), assuming constant electron temperature. γ_i is stabilizing and has negligable effect on ω_R values. Thus, both γ_e and λ_z are destabilizing. An increment of γ_i by an order of magnitude, i.e. decreasing either

γ_e or λ_z, reduces the growth rate by a factor of 20. The local slab model predicts more stable modes although the same values of ω_R are estimated by the two models.

Influence of magnetic field B is more complex, however a parameter β was used to simplify it where

$$\beta = (2e^2/QKT_e m_i)^{\frac{1}{2}}.B \tag{11}$$

and in the local model Q is replaced by $K_\perp^2$.

Values of ω_R and ω_I are indicated in Figures 9a and 9b as a function of β for typical parameters $m=2$, $\gamma_i = 6.4\times10^6$ sec^{-1} and $P = 10^{-4}$ torr when the non local model was applied. Lower values of ω_R and ω_I were predicted by the local model, however, both models produce two maxima at 1800 and 1000 gauss respectively provided that T_e remains constant. Thus, magnetic field is destabilized up to the maximum value of ω_I, then it becomes stabilized. Since the highest magnetic field used in the present experiment was 900 gauss, ω_I is expected to raise with B. This is in consistent with the appearance of definite mode at the definite magnetic field (while V_G remains constant). Increasing B caused the particular mode to disappear and another similar mode of different m and ω_R to be onset. Also, increase ω_R with magnetic field agree with the experimental data in Figure 5. On the other hand, electron temperature T_e is also destabilizing if the other operating parameters did not change. Values of ω_R and ω_I are enhanced remarkably by increasing T_e (Figures 9a and 9b). Since T_e increased by raising V_G the latter is destabilizing too.

Figure 10 shows a comparison between the measured and the computed

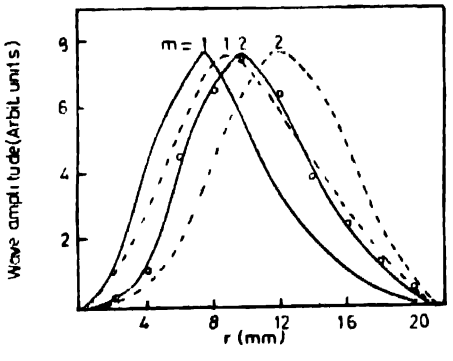

Figure 10. Radial wave amplitude distributions for $m=1$ and 2. Dotted curves, solid curves and (o) indicate bell shaped profile, Gaussian profile and experimental points, respectively.

waveforms at 600 gauss, for $m=1$ and $m=2$. The shape of the mode is very insensitive to the typical plasma parameter thus the radial distribution of the wave

amplitude was calculated using Ellis et *al* (1980) data beside the experimental results. The measured data was normalized to be equal to the theoretical predictions at the radial distance of maximum amplitude. A reasonable agreement is achieved with the bell shaped profile for $m=2$ mode (Figure 10). Only slight difference is observed with the Gaussian profile.

The experimental values of the drift wave frequency are compared with the values predicted by the full numerical model (Figure 11), after being corrects for the accocut of the Doppler shift. Measured plasma parameters and density profiles were used in the theoretical calculations. Only $m=2$ mode reveals reasonable

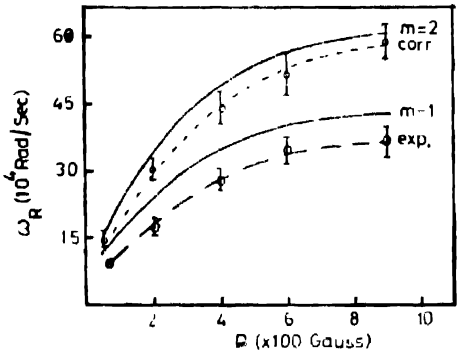

Figure 11. Comparison between the experimental (exp.) and corrected (corr.) values of (ω_R) and the thoeretical predictions.

agreement while $m-1$ mode is far below from the expected value. The measured frequency was chosen at grid potential $=40$ volts whereas constant values were recorded (Figure 5).

Finally, effect of the grid biased, on the stability of the plasma has been discussed. Firstly, it derives a weak current through the plasma beam. Secondly, an increase in V_a values produced higher T_e and U_0. Although it is difficult to quantize the exact effect of the electron current a qualitative explaination is given. Grid changes the axial boundary conditions in such a way that plasma becomes more unstable. Once the plasma has been destabilized, grid acts to govern the mode number and frequency of the drift wave. Increasing V_a is destabilizing as it result in increasing T_e and U_0, both of which proved to be strongly destabilizing parameters (Figures 7 and 9). Also at low magnetic field, and small V_a, the parameters, β, U_0 and λ_s are small. These parameters are also destabilizing. Thus the modes become unstable at low B only by raising V_a (i.e. increase B and U_0). However, at high fields B is large and ω_I is high enough to excite the mode regardless to the value of V_a (Figures 5–9).

4. Conclusion

Positive potentials have been applied to a grid in the path of a plasma flow in an axial magnetic field. Two fundamental functions of the D.C. bias are observed. Firstly, it produced secondary ionisation and excitation processes, thus increasing density and light output of the emerged plasma. The necessary threshold potential was found to be magnetic field dependent since the latter affects the probability of these processes. Secondly, it excites drift wave of different mode numbers and frequencies. The influence of the different governing parameters on the stability of the plasma, such as electron drift speed, parallel wave length of the wave, collision frequencies of electron and ion with neutral particles, magnetic field, electron temperature and grid potential, has been investigated theoretically, using the full numerical solution of the exact equation. It is concluded that it is the combination of these parameters that controls the stability of the definite measured mode. Effect of the grid has been explained on the bases of the electron current drawn in the plasma. Since both electron speed U_0 and electron temperature T_e are destabilizing, the grid positive potential is destabilizing. The parameter γ_i indicates stabilizing effect, and thus both electron-neutral collision frequency and the parallel wave length are destabilizing. On the contrary, the ion-neutral collision frequency is stabilizing. Other parameters remaining constant, magnetic field B is destabilizing only up to a certain value, after which it becomes stabilizing. Although the parameters U_0, γ_i and V_G (grid potential) have sligh effect on the values of the real frequency, the latter changed remarkably by T_e and B. We finally conclude that a reasonable agreement between the experimental data and the theoretical predictions may be obtained only when the full numerical solution is applied.

Acknowledgments

The author acknowledges the help and cooperation received from Prof M G Rusbridge and Dr K Phillips, Manchester University, Institute of Science and Technology. Thanks are also due to Dr A M Nossaair and to the group of plasma at Azhar University, Cairo, Egypt.

References

Bauwens G, Noblet A and Sylin G 1977 *Nucl. Instrum. Meth.* **143** 497

Brown S C 1967 *Basic Data of Plasma Physics* (Cambridg, Mass : The MIT Press) Ch 2

Cartier S L and Merlino R L 1984 *IEEE Transaction on Plasma Science* **Vol PS-12 No. 1** p 14

Chen F F 1965 *Plasma Diagnostic Technique* eds. Huddlestone R H and Leonurd S L (London : Academic) p 178

——1967 *Phys. Fluids* **10** 1647

——1974 *Introduction to Plasma Physics* (New York : Plenum)

Chu T K, Coppi B, Hendel H W and Perkins F W 1969 *Phys. Fluids* **12** 203

Delcroix J L 1968 *Plasma Physics Vol. 2 : Weakly Ionzed Gases* (New York : John Wiley)

Elakshar F F and Nossair A M 1984 *Egyptian Proc. Math. Phys. Soc.* **57** 75
Elakshar F F, Nossair A M and Phillips K 1985 *Indian J. Theor. Phys.* **38** 89
Ellis R F and Motley R W 1971 *Phys. Rev. Lett.* **27** 1496
——1974 *Phys. Fluids* **17** 582
Ellis R F and Marden B E 1977 *Bull. Am. Phys. Soc.* **22** 1088
Ellis R F and Marden-Marshall E 1979 *Phys. Fluids* **22** 2137
Ellis R F, Marden-Marshall E and Majeski R 1980 *Plasma Phys.* **22** 113
Golovanivskii K S 1971 *Sov. Phys. Tech. Phys.* **15** 1146
Ikazi H and Tayler R J 1970 *J. Appl. Phys.* **41** 738
Loeb L B 1956 *Handbuch der Physik* **Vol 21** (Berlin : Springer-Verlag) p 570
Marden B F, Ellis R F and Walsh J E 1978 *Bull. Am. Phys. Soc.* **23** 826
Massey H S W and Burhop E H 1969 *Electronic and ionic Impact Phenomena* **Vol I and II** (Oxford : Oxford Press)
Mitani K and Kubo H 1960 *J. Phys. Soc. Jap.* **15** 678
Okuda H and Dawson J M 1973 *Phys. Fluids* **26** 408
Self S A 1970 *Plasma Phys.* **4** 693
Swift J D and Schwar M J R 1970 *Electrical Probes for Plasma Diagnostics* (London : Iliffe Books)